An *in situ* ESR study of Pd/H-ZSM-5 interaction with different adsorbents

A.V. Kucherov [a,b] and M. Shelef [a]

[a] *Ford Research Laboratory, Ford Motor Company, MD 3179/SRL, PO Box 2053, Dearborn, MI 48121, USA*
E-mail: mshelef@ford.com
[b] *Zelinsky Institute of Organic Chemistry, Russian Academy of Sciences, Leninsky Prosp. 47, Moscow, Russia*
E-mail: lab14@ioc.ac.ru

Received 1 May 2001; accepted 31 May 2001

In situ ESR at 120–473 K permits to monitor formation of transient paramagnetic ions/complexes (isolated Pd^+ sites; Pd^+/H_2O; Pd^+/C_6H_6) upon interaction of isolated Pd^{2+} cations stabilized by the H-ZSM-5 matrix with different organic compounds and gas mixtures (NO, O_2, H_2O, H_2, propene, benzene). The *in situ* study provides insight into the elementary steps of redox processes on isolated Pd species in H-ZSM-5 zeolite under realistic conditions. Adsorbed water stabilizes the transient paramagnetic complex and decreases the rate of Pd^{2+} to Pd^0 reduction by H_2. Strong bonding of NO_x ligands to Pd^{2+} species suppresses the reduction of Pd(II) ions. Sorption of benzene on preoxidized Pd^{2+}/HZSM-5 is accompanied by an easy formation of organic cation-radicals and of a Pd^+/benzene complex, the paramagnetic Pd^+/benzene structure indicating a surprisingly high resistance to further reduction to Pd^0. Illumination of the Pd/HZSM-5 by UV-visible light causes no measurable change in the redox properties of the catalyst.

KEY WORDS: ESR; Pd/ZSM-5; redox properties; Pd^+ sites; NO_x; ligand stabilization

1. Introduction

Supported palladium is known as a component of three-way automotive catalysts, and has been studied by a wide variety of methods [1–4]. In the last 15 years paramagnetic Pd species formed in zeolites of different types (Y, X, L, Rho, SAPO) have also been examined by Kevan and his co-workers using ESR and electron spin echo modulation techniques [5–12]. Recently, in connection with the efforts to develop catalysts for NO reduction by methane in the presence of O_2, several attempts have been made to monitor the behavior of Pd sites on H-ZSM-5 and other acidic supports in the reduction of NO with CH_4 [13–16]. These methods were applied after the specimens were removed from reaction conditions and transferred into the respective characterization instruments and, hence, the information about the state of the catalyst *in situ* was arrived at indirectly, by inference. We have previously devised a direct method for *in situ* measurement of ESR-active ions under flow conditions and applied it to characterize specimens containing Cu^{2+} [17], Cr^{5+} [18], and Rh^{2+} [19,20].

Here, we extend this method to the *in situ* ESR study of the interaction of Pd/ZSM-5 with different inorganic and organic gaseous adsorbents and their mixtures (NO, O_2, CO, propene, H_2, benzene) at 120–473 K. Effect of the irradiation of the catalysts by UV-visible light was also monitored *in situ*.

2. Experimental

2.1. Samples

Two Pd/ZSM-5 samples, with 1.0 and 0.25 wt% Pd, were prepared by incipient wetness impregnation of NH_4-ZSM-5 (Si/Al = 25; PQ Corporation) by water solutions of Pd-ammino-nitryl complex (0.8 cm^3 per 1 g of dried zeolite). This compound was used to exclude the possible influence of Cl^- ligands being introduced by the use of more commonly employed $PdCl_2$.

The samples were pressed without binder, crushed into 0.1–0.2 mm particles and placed in a quartz ampoule for ESR measurements. Dried samples were precalcined at 500–800 °C in (He + 10% O_2) stream for 2–5 h.

2.2. ESR measurements

The ESR spectra of paramagnetic species, at 120–473 K, were taken in the X-band ($\lambda \approx 3.2$ cm) on a Bruker ESP300 spectrometer, equipped with a low-temperature cavity 4104 and a co-axial quartz gas flow cell [17]. Use of the cavity 4104 with optical slot permitted to combine *in situ* irradiation of the sample by UV-visible light with the ampoule cooling-heating from 120 to 473 K by flowing heated nitrogen. A mercury light source SP 200 (200 W) was used for the irradiation. A cylindrical quartz filter (6 cm length) filled with distilled water was used to cut off the IR-component of the spectrum to minimize sample heating by radiation. After absorption of the IR-component the beam was focused, on the ampoule inside the ESR cavity, by a quartz lens (spot diameter $\sim 1/2$ inch).

1011-372X/01/0800-0019$19.50/0

The Bruker ESP300E software and the special Bruker program WIN-EPR (version 901201) were used for data treatment (baseline correction, double integration, and deconvolution). The ESR signals were registered, at modulation of 2 G and microwave power of 6.4 or 64 mW, in the field region of 2700–3700 G (1024 points). Two modes of resonance registration were used: (1) two scans with a sweep time of ∼21 s; (2) ten scans with a sweep time of ∼42 s. The lack of sample saturation was verified for microwave power levels 0.64–64 mW.

A 25–30 mg charge of the catalyst was placed in a coaxial quartz flow ampoule with an inner diameter of ∼4 mm for ESR measurements [17]. This cell was placed into the ESR cavity and connected, by long stainless-steel capillaries with Teflon ferrules, to a gas flow system. This setup allowed baking of the cell in an outer high-temperature furnace at 500–800 °C and place it back into the 4104 cavity under gas flow. The gas flow, at pressure of ∼1 atm, was regulated by a four-channel readout mass flow controller (model 247C, MKS Instruments). This system permitted to change the composition of the gas mixture and to regulate the flow from 1.5 to 18 cm^3/min. Pure helium (99.999%) and the mixtures (10 vol% O_2 + He), (0.41 vol% NO + He), (0.39 vol% C_3H_6 + He), and (1 vol% H_2 + He) were used for *in situ* sample treatment. In some cases, the dynamics of the ESR signal change during interaction of the sample with H_2 was monitored at 20 °C; at a chosen moment the gas flow was stopped, the sample was cooled down to 120 K at a rate of ∼80°/min and the ESR signal from the frozen transient complex was taken as this temperature.

In experiments with benzene (chromatographically pure dry C_6H_6), the ampoule, with the sample charge (25–40 mg), was calcined at given temperature in air, taken out of the furnace, cooled, impregnated immediately with ∼0.3 cm^3 of liquid substance, evacuated for ∼30 s at 20 °C, and sealed off. Then the sample-containing ampoule was placed in the ESR cavity and cooled to 120 K by flowing nitrogen gas through a Dewar filled with liquid nitrogen.

3. Results and discussion

The matrix of high-silica ZSM-5 with metallic ions at a low loading stabilizes a high fraction of *isolated* ions as these are exchanged at the protonic sites. For low-loaded Cu^{2+}-ZSM-5 and Fe^{3+}-ZSM-5 samples virtually all copper or iron introduced are ESR-visible [21,22]. Quantitative evaluation of Rh^{2+} in ZSM-5 demonstrated that the fraction of ESR-visible isolated ions exceeds 50% for the most dilute 0.25% Rh/ZSM-5 [20]. Hence, the Pd-containing samples prepared with the use of the same H-ZSM-5 may also be used for *in situ* ESR study of interaction between mononuclear Pd active sites and different molecules under realistic conditions.

Pd^{3+} and Pd^{+} oxidation states of palladium species ($4d^7$ and $4d^9$ electronic configurations, respectively) show paramagnetic properties, and the ESR pattern of Pd^{+} generally differs drastically from that of Pd^{3+}. Pd^{+}-ESR signal is characterized by a large anisotropy of the g-tensor with $g_\perp < g_\parallel$, whereas an isotropic signal at $g \approx 2.23$ or a signal with small anisotropy and $g_\perp > g_\parallel$ are typical of Pd^{3+}. The most common Pd^{2+} oxidation state is ESR silent but formation of paramagnetic complexes, such as (Pd^{2+}–O_2^-), gives rise to appearance of the ESR signal with a relatively small anisotropy and $g_\perp > g_\parallel$.

3.1. Paramagnetic Pd species in oxidized Pd/ZSM-5

The Pd/ZSM-5 sample was calcined at 600–720 °C in (10% O_2 + He) flow for 2 h. Then the gas flow was switched to pure He at high temperature, the ampoule cooled to room temperature in He flow and placed into the ESR cavity. A rather weak ESR signal from this pre-oxidized sample, with $g_\perp = 2.046$ and $g_\parallel = 1.989$, is shown in figure 1(a). The same signal was observed when pre-oxidized sample was cooled to 20 °C in (10% O_2 + He) flow and purged with pure He at room temperature. The signal (figure 1(a)) is typical of paramagnetic (Pd^{2+}–O_2^-) complex observed for different types of zeolites [5–9]. However, this intensity of this signal can be responsible for a minor part only (1–3%) of the palladium ions introduced into the zeolite. This is consistent with most of the palladium in oxidized PdH-ZSM-5 being present as Pd^{2+} cations [3,13].

When the gas flow is switched back to (10% O_2 + He) flow at 20 °C, an immediate broadening of the ESR signal from admixture of (Pd^{2+}–O_2^-) complex takes place, as shown in figure 1(b). Repeat purging of the sample by pure He results in complete restoration of the starting signal (figure 1(a)). Therefore, paramagnetic Pd species in pre-oxidized Pd/HZSM-5 undergo dipole–dipole interaction with O_2 molecules from the gas phase.

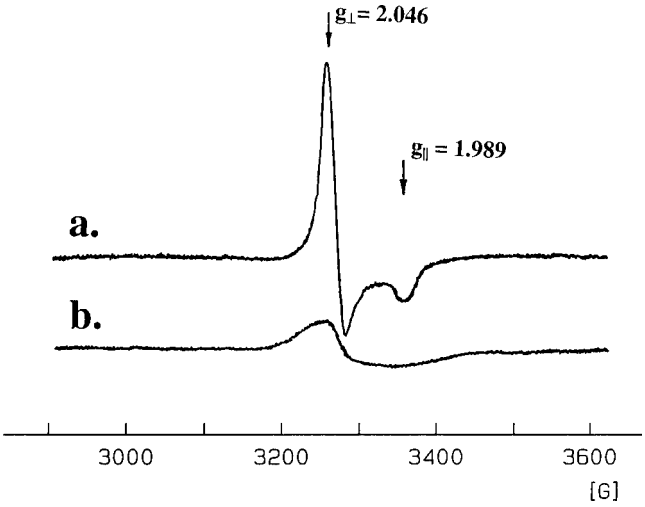

Figure 1. ESR spectra, at 20 °C, of Pd/HZSM-5 calcined at 700 °C: (a) in He flow and (b) in (10 vol% O_2 + He) flow.

3.2. Interaction of Pd/ZSM-5 with NO, H_2O, C_3H_6, and C_6H_6

ESR signal intensity from oxidized Pd/ZSM-5 (figure 1(a)) depends strongly on the presence of different adsorbate molecules.

Treatment of the sample at 20 °C with a flow of (He+NO) is accompanied by gradual, irreversible and complete loss of the signal intensity (figure 2). Illumination of the sample with UV-visible light has no effect on the kinetics of disappearance of paramagnetic species, as shown in figure 3. The treatment does not cause any change of the original, light-brown sample color, typical of Pd^{2+}-containing samples.

Treatment of the sample at 20 °C with a flow of He saturated with water vapor is also accompanied by a gradual irreversible decrease of the ESR signal intensity (figure 3, dotted line). No change in the original, light-brown, sample color is seen after water adsorption.

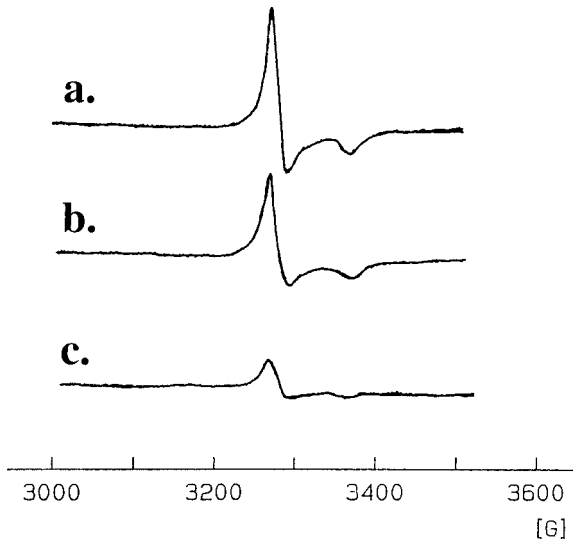

Figure 2. *In situ* ESR spectra at 20 °C of oxidized Pd/ZSM-5: (a) in He flow, (b) (He + NO) flow 3 min and (c) (He + NO) flow 10 min.

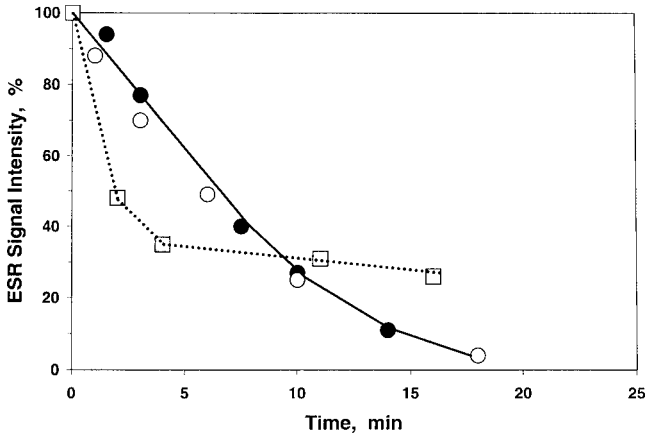

Figure 3. Kinetics of ESR spectrum intensity change upon interaction of oxidized Pd/ZSM-5 at 20 °C: (•) (He + NO) flow, no light; (○) (He + NO) flow, UV-visible illumination; and (□) (He + H_2O) flow.

Propene chemisorption on oxidized Pd/HZSM-5 causes gradual ESR signal loss, and kinetics of this process is shown in figure 4. Heating of the sample with propene at 100 °C for 30 min is not accompanied by ESR signal appearance. At the same time, the sample changes color to dark-gray being typical of reduced Pd^0-containing catalysts.

Thus, interaction of oxidized Pd/HZSM-5 with the abovementioned compounds does not cause formation of new stable paramagnetic species from Pd^{2+} sites but destroys the stabilized (Pd^{2+}–O_2^-) species.

Study of benzene interaction with Pd/HZSM-5 demonstrates the formation/stabilization of paramagnetic Pd^+–C_6H_6 species at 20–200 °C. All cationic positions in H-ZSM-5 are accessible for benzene in the zeolitic channels. Impregnation of Pd/ZSM-5 with benzene at 20 °C results in the appearance of an ESR signal (figure 5(a)) strongly differing from the starting spectrum (see figure 1(a)). Evacuation of the impregnated sample at 20–100 °C is not accompanied by a change in the spectrum, and no change in the signal shape is observed upon cooling from room temperature to 120 K. Heating the sample at 200 °C for 1 h results in a ∼1.5-fold increase in the ESR signal intensity without any change in the spectrum shape (figure 5(b)). Only further calcination at 300 °C for 30 min causes the complete disappearance of the ESR signal shown in figure 5. At the same time, an intense narrow ESR singlet ($g = 2.0036$, $\Delta H = 10$ G) from "coke" residue is formed, and the sample becomes black. Thus, the formation of a surprisingly strong and stable paramagnetic complex takes place during the interaction of Pd/ZSM-5 with C_6H_6 molecules. The ESR signal, with $g_1 = 2.52$, $g_2 = 2.22$, and $g_3 = 2.10$, shown in figure 5, is typical of paramagnetic Pd^+–C_6H_6 species stabilized in different zeolitic matrixes [5,6,9,12]. The integral intensity of the ESR spectrum formed (figure 5(b)) exceeds the intensity of the rather weak starting signal (figure 1) by two–three orders (!) of magnitude. Thus, the *main* part of ESR-silent Pd^{2+} species is transformed into paramagnetic (Pd^+–C_6H_6) complexes by benzene interaction with oxidized Pd/HZSM-5. This can be taken as an indirect evidence

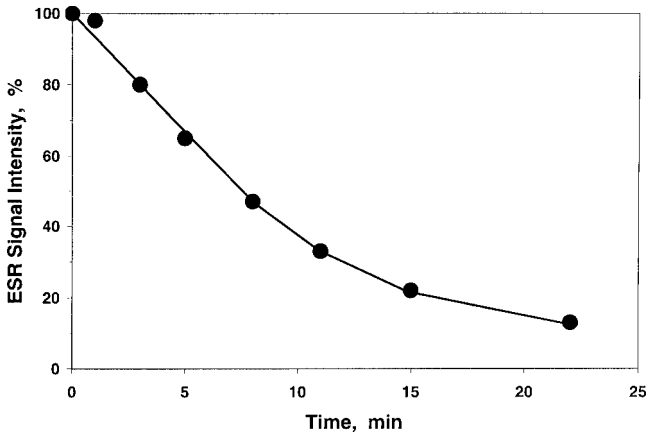

Figure 4. Kinetics of ESR spectrum intensity change upon interaction of oxidized Pd/ZSM-5 with propene at 20 °C in He flow.

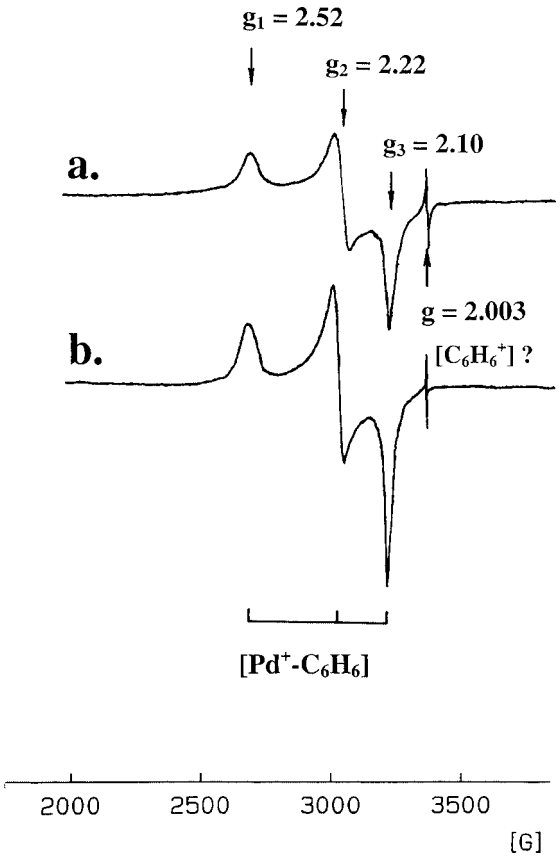

Figure 5. ESR spectra at 120 K, of Pd/HZSM-5 calcined at 700 °C: (a) after impregnation with liquid benzene at 20 °C and evacuation; and (b) after heating at 200 °C for 1 h.

of the mononuclear nature of the starting Pd^{2+} active sites in our samples.

The high stability of paramagnetic mononuclear Pd^{+}–benzene complexes against further reduction is surprising, because interaction of the same Pd/HZSM-5 with H_2 at room temperature is accompanied by an easy reduction of Pd^{2+} to Pd^0. Kinetics of this reaction will be discussed below. C_3H_6 adsorption also causes reduction of palladium ions to metal at $T \leqslant 100$ °C. One can assume that it could be related to differences in the chemical nature of the transient species. It appears that the benzene molecules effectively inhibit further reduction of the (Pd^{+}–C_6H_6) adducts formed in H-ZSM-5 channels. The formation of isolated paramagnetic complexes stabilized by benzene molecules was also noted earlier in the Rh/HZSM-5 system [20].

At the same time, the charge transfer to benzene molecules, with the formation of stable cation-radicals, is of relatively minor importance, as distinct from the case of Cu^{2+} reaction with benzene in CuH-ZSM-5 [23]. Interaction of the reactive square-planar Cu^{2+} ions with benzene at 20 °C is accompanied by copper reduction with formation of stable $C_6H_6^{+}$ cation-radicals, as confirmed by appearance of the intense characteristic ESR spectrum with $g \approx 2.002$ [23]. A signal of this type is relatively weak in the interaction of benzene with Pd/ZSM-5 (figure 5).

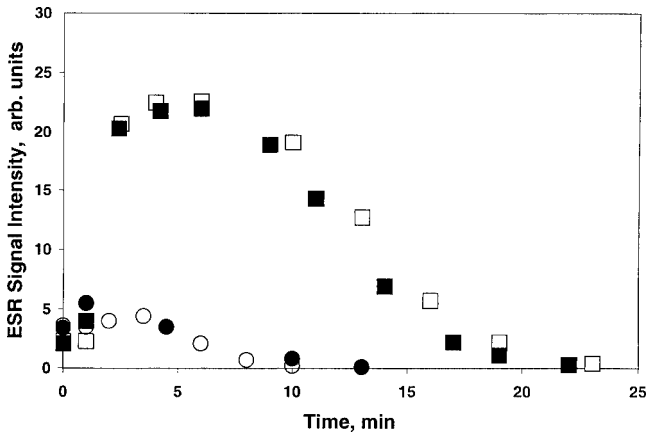

Figure 6. Kinetics of ESR spectrum intensity change upon interaction of pre-oxidized Pd/ZSM-5 with (He + 1% H_2) flow at 20 °C: (1) purged with He at 600 °C (•) no light, (○) UV-visible illumination); (2) purged with He at 20 °C (■) no light, (□) UV-visible illumination).

3.3. In situ ESR monitoring of reduction–oxidation of Pd/ZSM-5

In situ monitoring of isolated paramagnetic Pd species in a flow of reactants allows one to specify the state of active sites in supported Pd catalysts under conditions closer to those of a working catalyst.

3.3.1. Dynamics of Pd/ZSM-5 reduction by H_2 in presence of O_2 or H_2O sorbed

Dynamics of the ESR signal change accompanying the treatment of Pd/ZSM-5 with H_2 at room temperature depends strongly on the sample pretreatment conditions. Purging the Pd/ZSM-5 by He flow at either 600 °C or at room temperature, after oxidative calcination, results in the same starting, weak (Pd^{2+}–O_2^{-}) ESR signal (figure 1(a)). However, these two samples, which differ in the amount of weakly-bonded molecular oxygen, demonstrate different behavior upon subsequent reduction.

Pd/ZSM-5 purged with He at high temperature. Treatment of this sample at 20 °C with a flow of (He + H_2) is accompanied by gradual, irreversible and complete loss of the ESR signal intensity in less than 12 min. The treatment causes change of the original, light-brown, sample color to dark-gray one being typical of Pd^0-containing samples. Thus, irreversible reduction of isolated Pd^{2+} ions in H-ZSM-5 by hydrogen takes place easily at room temperature, the second step of transformations $Pd^{2+} \rightarrow Pd^{+} \rightarrow Pd^0$ is fast, and no accumulation of transient paramagnetic Pd^{+} species can be detected. Irradiation of the sample with UV-visible light has no effect on the kinetics of disappearance of paramagnetic species. Dynamics of the signal loss is shown in figure 6 (curve (1), circles).

Reduction of *Pd/ZSM-5 purged with He at room temperature* is accompanied by a different sequence of the ESR signal transformations. Switching the gas flow to (He + H_2) induces an immediate change in the signal shape, with a fast 5–6-fold increase of the integral intensity. Maximum intensity

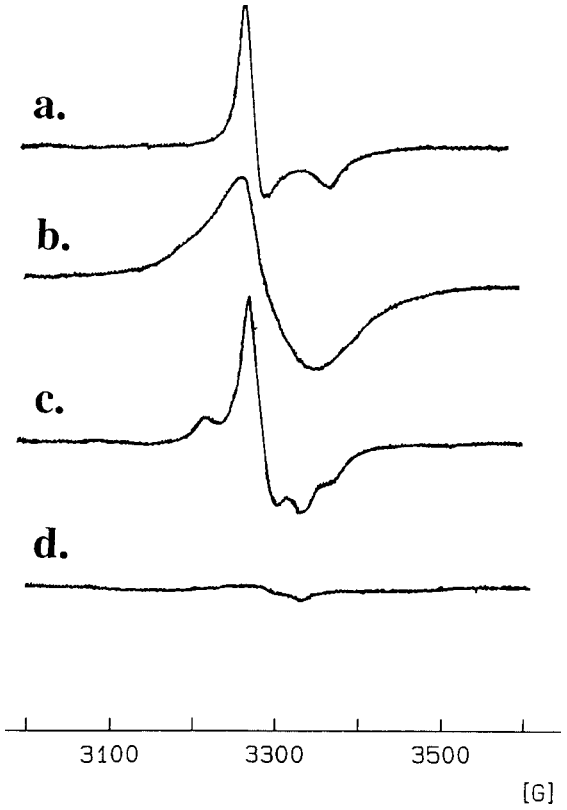

Figure 7. ESR spectra of Pd/HZSM-5 taken, at 120 K, on different steps of the sample reduction by H_2 at 20 °C: (a) starting signal; (b) after ∼4 min of treatment; (c) after ∼10 min of treatment; (d) after ∼17 min of treatment.

of the signal is reached in 5–6 min, and further treatment of the sample with a ($He + H_2$) flow is accompanied by a gradual irreversible loss of the ESR signal. Finally, the sample color becomes dark-gray. Kinetics of change of the integral ESR intensity is shown in figure 6 (curve (2), squares). UV-visible light has no measurable effect on the kinetics of formation/disappearance of paramagnetic species. ESR spectra taken on different steps of the sample reduction *in situ* with H_2 at 20 °C are presented in figure 7. *Pd/ZSM-5 sample with preadsorbed water* demonstrates a similar volcano-shape change of ESR signal upon H_2 treatment. Our method of measurement of the weak ESR signals is quite slow, with averaging of the ESR signal during ∼40 s of measurement, but for the process lasting ∼20 min (figure 6) it permits to monitor kinetics of accumulation/decomposition of the transient paramagnetic species quite well.

Thus, water preadsorbed, or formed *in situ*, on isolated Pd^{2+} ions in H-ZSM-5 stabilizes the transient paramagnetic complex and decreases noticeably the rate of irreversible reduction $Pd^{2+} \rightarrow Pd^{+} \rightarrow Pd^{0}$ by H_2. As a result, a considerable temporary accumulation of transient paramagnetic species can be detected due to retardation of the second step of the process.

3.3.2. Reoxidation of reduced Pd/ZSM-5

Treatment of prereduced samples by ($He + O_2$) flow was studied *in situ* at 20–280 °C. No formation of paramagnetic species was detected both in the dark and with illumination. Color and adsorption properties of the sample oxidized at 280 °C were not identical to those of the starting sample. Oxidative calcination at 600–700 °C completely restores the original properties of the Pd/ZSM-5 samples.

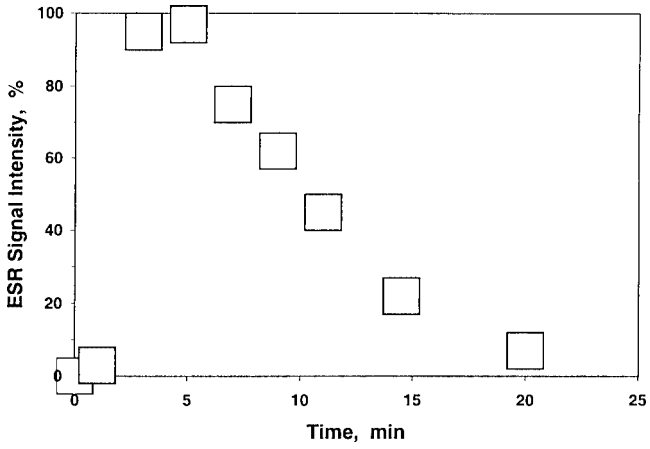

Figure 8. Kinetics of ESR spectrum intensity change upon interaction of Pd/ZSM-5, saturated with NO at 20 °C and purged with He flow at 280 °C, with ($He + 1\%\ H_2$) flow at 20 °C.

3.3.3. Peculiarities of Pd/ZSM-5 reduction by H_2 in presence of adsorbed NO

Influence of preadsorbed NO. Sorption of NO on the sample at 20 °C causes irreversible and complete loss of the ESR signal, as mentioned before (figure 2). Switching the gas flow, at 20 °C, to pure He and then to ($H_2 + He$) does not reduce the sample. No change of the sample color is noted. Removal of a weakly bonded part of the adsorbed NO, by purging the sample with He flow at 60 °C for 15 min, does not increase the reducibility of the inhibited sample: no reduction by hydrogen at room temperature takes place. Conversely, a complete restoration of Pd/ZSM-5 reducibility by hydrogen (figure 6, curve (1)) occurs after the sample purging with He flow at 450 °C.

Removal of NO under milder conditions, with He flow at 280 °C for 15 min, produces a sample with interesting reduction dynamics. Changes of the ESR signal intensity accompanying the interaction of such Pd/ZSM-5 with H_2 at 20 °C are shown in figure 8. After the induction period of ∼5 min, a fast accumulation of paramagnetic Pd^{+} species takes place, with subsequent relatively slow step of the irreversible loss of these paramagnetic sites. The sample finally becomes dark-gray. Kinetics of the process (figure 8) corresponds to accumulation/loss of the intermediate in an autocatalytic reaction $Pd^{2+} \rightarrow Pd^{+} \rightarrow Pd^{0}$. One can assume that the reduction starts with a relatively small part of Pd^{2+} sites, free of strong ligands, and the Pd^{0} formed activates the H_2 for further reduction of the less reactive sites. Because of the delay in the second reduction step, a measurable transient accumulation of paramagnetic species can be detected even with our relatively slow method.

3.4. In situ sample treatment in flowing gas mixtures (H_2 + NO) at 200 °C

The Pd/ZSM-5 sample shows no ESR signal in (0.4% NO + He) flow at 200 °C. No transformation of the catalyst occurs when the gas flow is switched to (NO+H_2+He) mixture with NO/H_2 ratio of 3/2. Under overall *reducing* conditions, with an NO/H_2 ratio of 2/3, the catalyst also remains unchanged. However, switching to a pure (1% H_2+He) flow results in a fast and irreversible reduction of the catalyst. The process at 200 °C is too fast (<2 min) to be monitored by ESR of the transient Pd^+ state.

4. Concluding remark

Preadsorption of NO on isolated Pd^{2+} ions in H-ZSM-5, *i.e.*, strong bonding of NO_x ligands to Pd^{2+} species, suppresses the reducibility of Pd(II) sites. Even the desorption of NO at 280 °C does not restore the original reactivity of the sites, and the retained part of strongly bonded NO is able to retard the irreversible reduction $Pd^{2+} \rightarrow Pd^+ \rightarrow Pd^0$. The effect can be even stronger when NO is present as a component of the gas flow. The strong inhibiting effect of NO on the reducibility of palladium ions has to be taken into account when reactions with NO_x participation are investigated on Pd-containing zeolite catalysts.

References

[1] A. Fritz and V. Pitchon, Appl. Catal. B 13 (1997) 1.
[2] I.N. Filimonov, I.A. Ikonnikov and A.Yi. Loginov, J. Chem. Soc. Faraday Trans. 90 (1994) 219.
[3] A.W. Aylor, L.J. Lobree, J.A. Reimer and A.T. Bell, J. Catal. 172 (1997) 453.
[4] A. Ali, W. Alvarez, C.J. Loughran and D.E. Resasco, Appl. Catal. B 14 (1997) 13.
[5] J.-S. Yu, C.W. Lee and L. Kevan, J. Phys. Chem. 98 (1994) 5736.
[6] J.-S. Yu, J.-M. Comets and L. Kevan, J. Chem. Soc. Faraday Trans. 89 (1993) 4397.
[7] G.-H. Back, J.-S. Yu, V. Kurshev and L. Kevan, J. Chem. Soc. Faraday Trans. 90 (1994) 2283.
[8] J.-S. Yu and L. Kevan, J. Chem. Soc. Faraday Trans. 91 (1995) 3987.
[9] J.-S. Yu and L. Kevan, Langmuir 11 (1995) 1617.
[10] M. Hartmann and L. Kevan, J. Phys. Chem. 100 (1996) 4606.
[11] M. Narayana, J. Michalik, S. Contarini and L. Kevan, J. Phys. Chem. 89 (1985) 3895.
[12] C.W. Lee, J.-S. Yu and L. Kevan, J. Phys. Chem. 96 (1992) 7747.
[13] L.J. Lobree, A.W. Aylor, J.A. Reimer and A.T. Bell, J. Catal. 181 (1999) 189.
[14] C.J. Loughran and D.E. Resasco, Appl. Catal. B 5 (1995) 351.
[15] C.J. Loughran and D.E. Resasco, Appl. Catal. B 7 (1995) 113.
[16] A. Ali, Y.-H. Chin and D.E. Resasco, Catal. Lett. 56 (1998) 111.
[17] A.V. Kucherov, J.L. Gerlock, H.-W. Jen and M. Shelef, J. Phys. Chem. 98 (1994) 4892.
[18] A.V. Kucherov, C.P. Hubbard and M. Shelef, Catal. Lett. 33 (1995) 91.
[19] A.V. Kucherov, S.G. Lakeev and M. Shelef, Appl. Catal. B 16 (1998) 245.
[20] A.V. Kucherov, S.G. Lakeev and M. Shelef, Micropor. Mesopor. Mater. 20 (1998) 355.
[21] A.V. Kucherov, H.G. Karge and R. Schlögl, Micropor. Mesopor. Mater. 25 (1998) 7.
[22] A.V. Kucherov and M. Shelef, J. Catal. 195 (2000) 106.
[23] A.V. Kucherov and A.A. Slinkin, Kinet. Katal. 38 (1997) 768.